PROCEEDINGS, 48th Workshop on Geothermal Reservoir Engineering
Stanford University, Stanford, California, February 6-8, 2023
SGP-TR-224

Serendipitous Petrothermal-Reservoir Development in a Region with Ascertained Large-Scale Hydrothermal Resources

Horst Behrens, Julia Ghergut, Martin Sauter

Applied Geoscience Dept., Goldschmidtstr. 3, University of Göttingen, 37077, Germany

iulia.ghergut@geo.uni-goettingen.de

Keywords: temperature decline, thermal drawdown, tracer test, inter-well, matrix diffusion, joint inversion, single-fracture model, petrothermal, Malm aquifer, Molasse basin, Alpine foreland

ABSTRACT

We deal with a particular well doublet in a porous-fissured-fractured formation ('Malm aquifer') that had been assessed as very promising and expected to provide for hydrothermal-reservoir operation at commercial levels for at least four decades, but whose conspicuous decline of production temperature has raised suspicion of a flow-path shortcut between injection and production locations. Various hypotheses on the hydrogeological nature of possible shortcut features, and on their geometry and size have been examined by Behrens et al. (2020, 2021[a]).

Eventually, tracer signals as recorded until 2022 yield unambiguous evidence for the presence of a misaligned large-scale fault zone (which has remained undetected by prior geophysical exploration) connecting the injection and the production well, and enable to quantify its transport-effective aperture, 15–20 cm, and fluid-swept area, ~10 million m². Such large sizes are incompatible with the previously considered scenario of a misaligned fracture induced by early-time stress-field rotation (a poroelastically coupled effect of fluid circulation onset, with the well doublet behaving like a strike-slip source mechanism).

Owing to the petrothermal behavior thus ascertained, production temperature decline rates are likely to significantly dwindle over the next decade; production temperatures would not drop below 95°C for at least 35 years under the current operation scheme.

It looks somewhat spectacular to find such markedly petrothermal behavior in a reservoir play setting known as hydrothermal-par-excellence (Germany's best hydrothermal region, by the current state of knowledge). Moreover, this unintended petrothermal-reservoir development appears to be the most successful (!) among all petrothermal systems whose development was attempted in Germany so far. Along with certain non-standard findings from other sites in the Alpine foreland basin, like Geretsried (Moeck et al. 2020), St. Gallen (Swiss Molasse Basin), and Kirchweidach in North-Eastern Bavaria, it sheds a new light on carbonate-petrothermal prospects which might become worth dedicated exploration in the future.

1. INTRODUCTION

Is the expansive deployment of inter-well circulation-based geothermal projects in Malm formations beneath the Greater Munich Area (in the SE-German region of the Molasse Basin) sustainably scalable? To answer this question, the German federal govt.-funded project "TRENDS" (cf. Behrens et al. 2020, 2021[a]) set out to

1° scrutinize the hydrogeology of Malm aquifers with a focus on fluid transport parameters (transport-effective porosity, dual-porosity features, fluid-rock interface area density) and on the facies-specific void-space structure at geothermal operation scales, using multi-tracer techniques of inter-well or single-well design (fig. 1),

2° quantify fluid flow, predict heat transport under various scenarios for the future deployment and exploitation of Malm aquifer-based geothermal resources,

3° identify critical restrictions to reservoir exploitation resulting from either hydraulic or geothermal heat supply 'competition' effects between 'neighboring' reservoirs.

While it is beyond doubt that 2° and 3° cannot be achieved without using some fluid-based tracking procedure (cf. Horne 1985), viz. tracer tests, the use of artificial tracers is challenged by the very large size of Malm reservoirs in the Molasse Basin, implying long residence times of circulating fluids, and strong dilution of tracers therein (cf. Behrens et al. 2021[b], Ghergut et al. 2015). As a workaround, we propose 'nil signal' interpretation approaches for early inter-well test stages. As a complement at mid-late inter-well test stages, we propose efficient single-well push-pull techniques relying on 'endo-tracers' (cf. Ghergut et al. 2019). We coined the term 'endo-tracer' to describe tracers whose (more or less remote-)past input into georeservoir fluid had been like that of an artificial tracer with one-time input at a circumscribed location, but whose current spreading in the circulating fluid resembles more the natural-tracer pattern (i. e., quasi-uniform spreading over sufficiently large space and/or time intervals – 'sufficiently' w. r. to the desired application scale). Lastly, we deal with a particular well doublet in a 'Malm aquifer' that had been assessed as very promising and expected to provide for hydrothermal-reservoir operation at commercial levels for at least four decades, but whose conspicuous decline of production temperature has raised suspicion of a flow-path shortcut between injection and production locations.

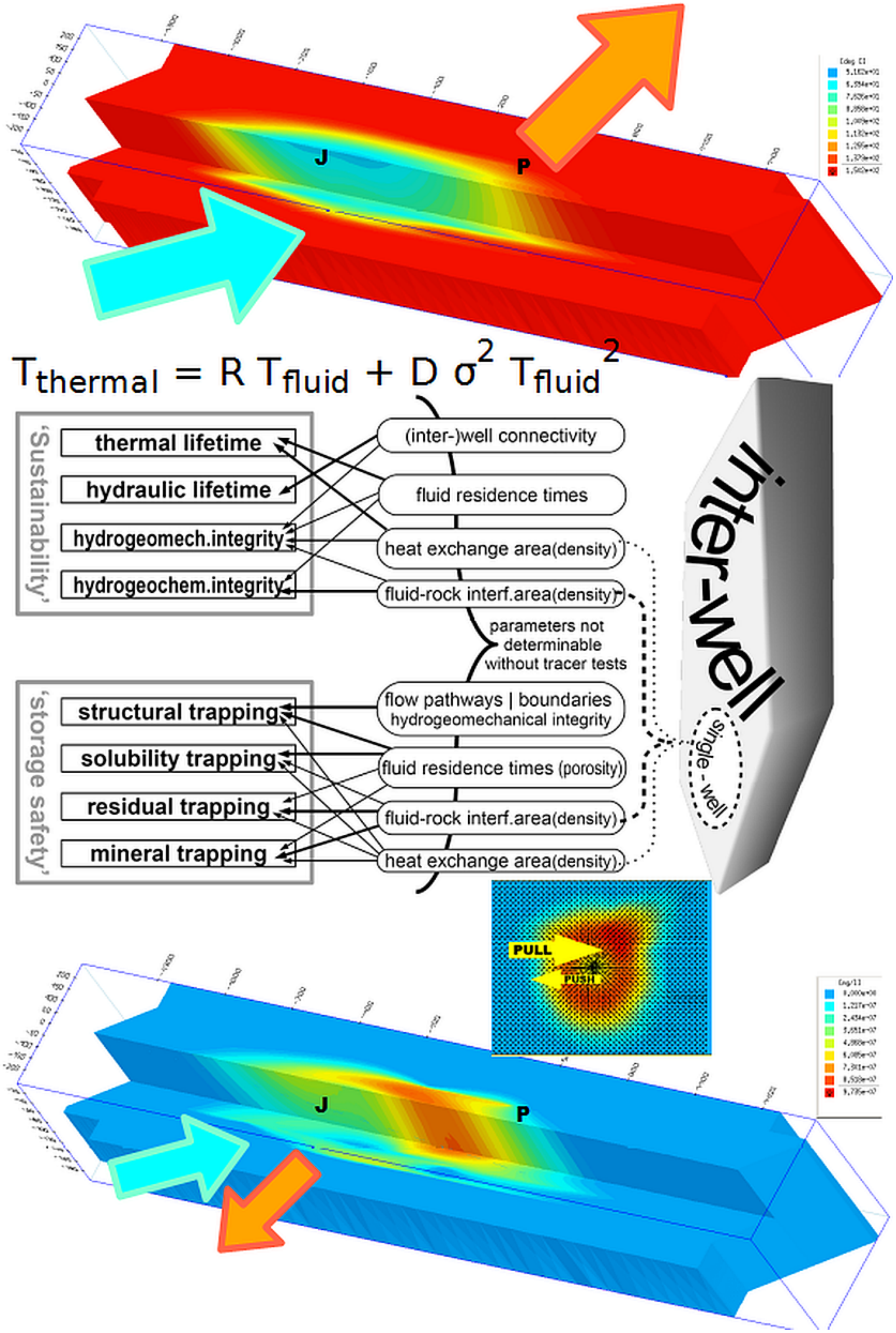

Figure 1: Reservoir features, properties, and parameters, whose quantification is endeavored by inter-well (multi-well) and/or single-well tracer tests, aiming to assess the so-called 'sustainability' of mid- and long-term exploitation for geothermal reservoirs, or deep geological storage formations, etc.

Various hypotheses on the hydrogeological nature of presumed shortcut features, and on their geometry and size have been examined in previous studies (cf. fig. 3 of Behrens et al. 2021[a], fig. 2 of Behrens et al. 2020). Assessing flow-path shortcut effects solely in terms of fluid advection (fig. 7 of ibid.) leaves the correlation between fluid residence time and thermal lifetime largely inconclusive.

2. JOINT INVERSION OF PRODUCTION TEMPERATURE AND SOLUTE TRACER SIGNALS

Motivated by the geothermal plant operator's perception of 'unexpected trends' in production temperature evolution, the 'tracer method' implementation focus thus moved from a tracer-assisted prediction of heat mining performance towards a joint inversion of measured tracer and production temperature signals, i. e. from

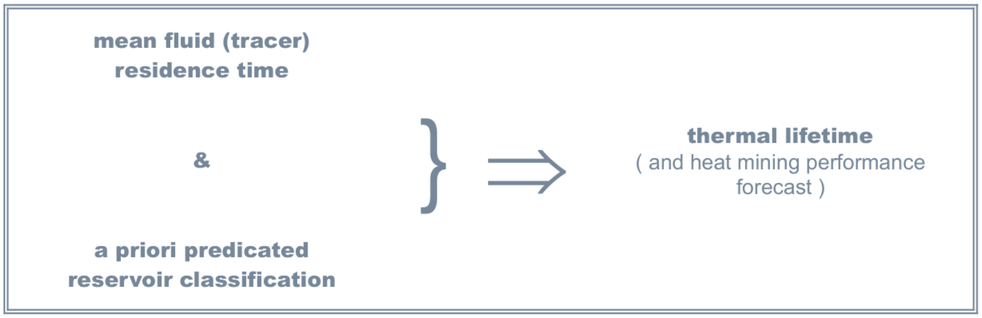

towards

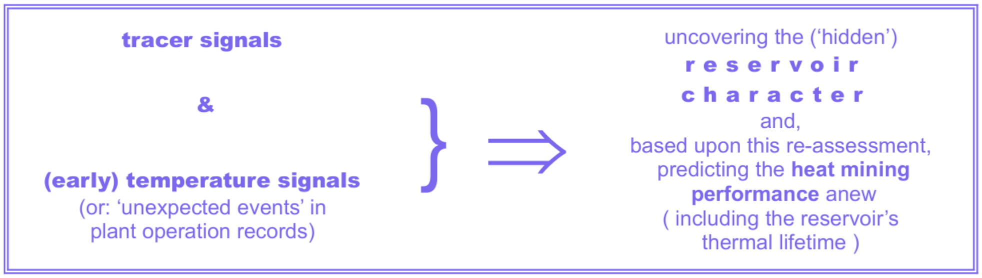

This method focus shift is also reflected by a relocation in the lifetime diagram (fig. 2).

Eventually, tracer signals measured to date (fig. 3) yield unambiguous evidence for the presence of a misaligned large-scale fault zone (which has remained undetected by prior geophysical exploration) connecting the injection and the production well, and enable to quantify its transport-effective aperture, 15–20 cm, and its fluid-swept area, ~10 million m^2. Such large sizes, independently corroborated (figures 2 and 3) by joint inversion of temperature and dual-solute tracer signals, are incompatible with the previously considered scenario of a misaligned fracture induced by early-time stress-field rotation (a poroelastically coupled effect of fluid circulation onset, with the well doublet behaving like a strike-slip source mechanism, cf. figures 8 – 12 in Behrens et al. 2020).

Fig. 3 summarizes the outcome of parameter inversion by 'fitting' a single-fracture model to the measured tracer signals, 'fitting' values being sought for three mutually-independent parameters: mean residence time (MRT), Péclet number (Pe), lateral exchange number (MxDiff, an aggregate dimensionless parameter quantifying the effects of transversal matrix diffusion fluxes, scaled by longitudinal advection fluxes). Measured tracer signals are shown in deconvolved (cf. fig. 1 in Behrens et al. 2021) and re-scaled shape; time scaling by MRT differs between plot rows, which renders signal shapes 'accelerated' or 'decelerated' (besides the effects of Pe and MxDiff),

► (l.-h.s.) in dark blue for the 'old' tracer, which has been added during a lower-rate flow regime (cf. Behrens et al. 2021),

► (r.-h.s.) in light blue for the 'new' tracer, added about 21 months later during a higher-rate flow regime, implying stronger dilution.

Model-fitted (simulated) signals are shown in cyan, parameter inversion results being summarized in plot legends accordingly. Signals in gray were simulated with identical values for MRT and Pe, but with MxDiff = 0, corresponding to advective-dispersive transport without matrix diffusion. Finding them to deviate considerably from the true (measured) signals endorses the significant role of the 'hidden' fracture, matrix diffusion effects appearing to be non-negligible even at early signal stages (which contravenes the widespread expectation "*matrix diffusion can be neglected in short-term tests*"). The cumulative tracer recovery ratio for each tracer transport scenario is shown by dashed curves in pairwise-similar color (with axis values in percent at the r.-h.s. to each plot).

Non-monotonous (tailing slope drop & recovery) episodes in the measured signals were induced by short-term tracer-free fluid slug injections in the context of wellbore treatments (marked in yellow). If certain requirements are met, the 'episodic' segment of tailing recovery can be evaluated quantitatively, more or less similarly to a (dual-tracer) single-well push-pull test; in this case, the gently sloping late-time tailings of the two artificial tracers perform in guise of two genuine 'endo-tracers' (Ghergut et al. 2019).

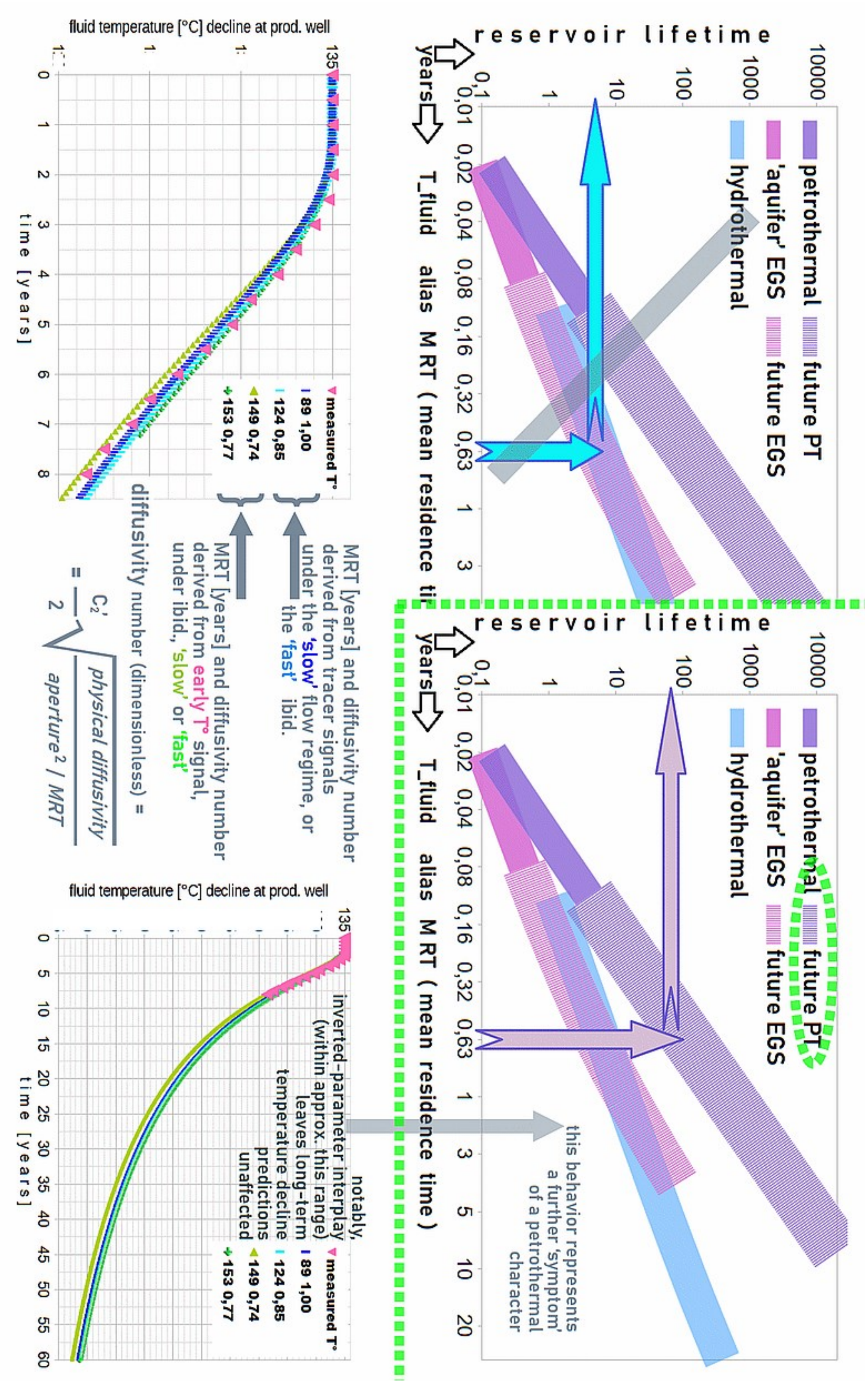

Figure 2: Workflow for a tracer-based re-assessment of the true reservoir character (identifying it as petrothermal-type), and overview of target reservoir parameters (to be identified by joint inversion of temperature and solute tracer signals).

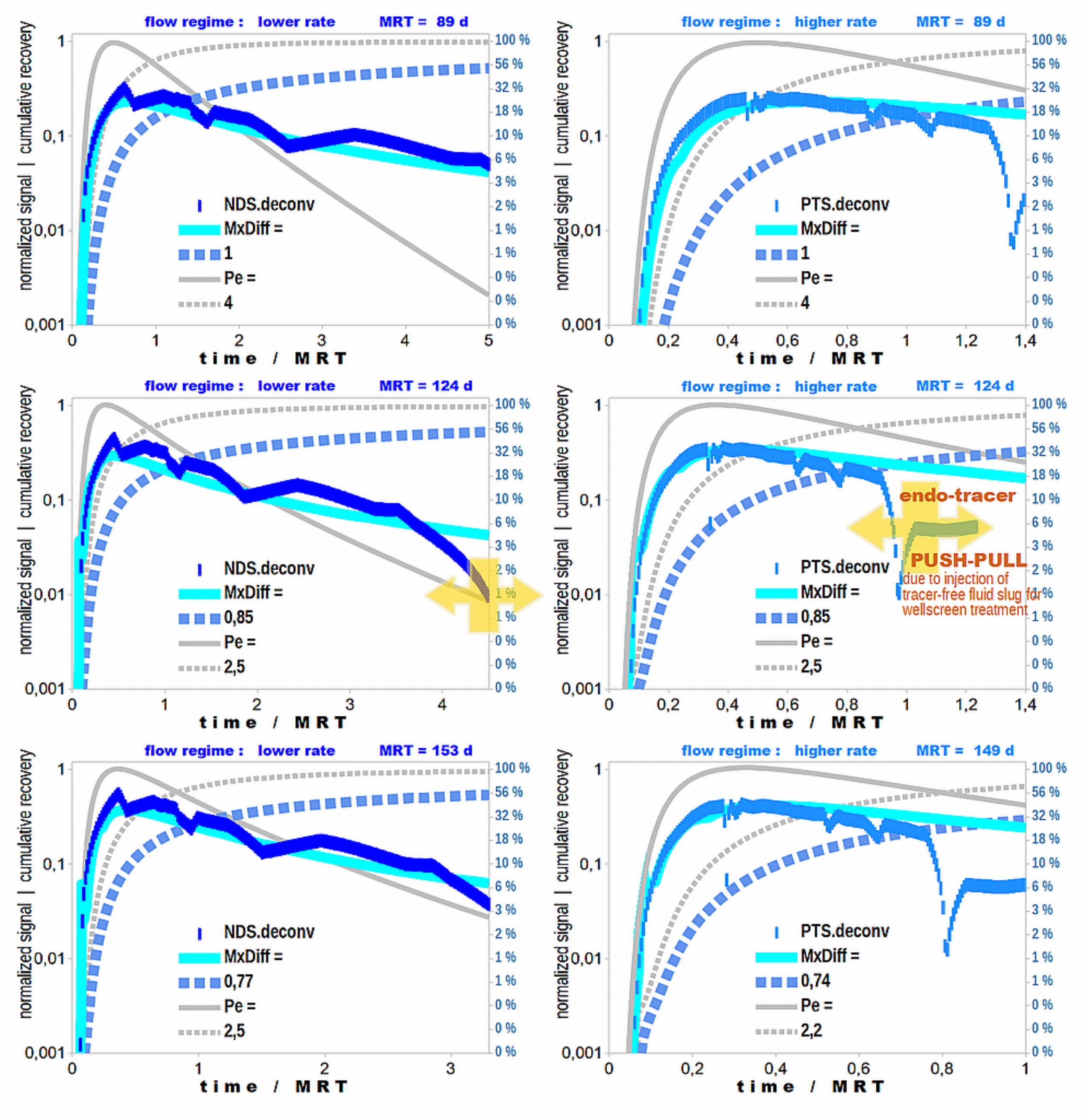

Figure 3: Reservoir parameter inversion by 'fitting' a single-fracture model to the measured tracer signals.

Further, figure 4 illustrates some 'heat mining' effects of large-scale fractures or fault zones striking transversely (or obliquely) to the inter-well axis, assessed individually by their relative distance between production and re-injection wells. Such 'well-aligned faults' had been documented by prior seismic exploration at the geothermal project site under investigation, and were also incorporated in the distributed-parameter model of Behrens et al. 2020 (cf. dashed lines in white in fig. 2 of ibid. at top row middle).

In fig. 4 below, one can compare between a reservoir with five 'active' well-aligned fractures (or fault zones), and reservoir instances in which one such fracture is missing (or 'closed'). In spite of apparently quite contrasting temperature distribution patterns in vertical sections along the fracture planes, temperature evolution at the production well remains almost unchanged, regardless of the presence (and hydraulic properties) of 'well-aligned' fractures. Thus, the governing process remains thermal drawdown along the inter-well axis, which is controlled by the longitudinal (shortcut) fracture. This further implies that additional 'observation wells' incidentally intersecting some transverse fracture or fault zone might fail to provide an adequate picture of reservoir-scale cooling. This, again, endorses the major role of the 'hidden' longitudinal fracture.

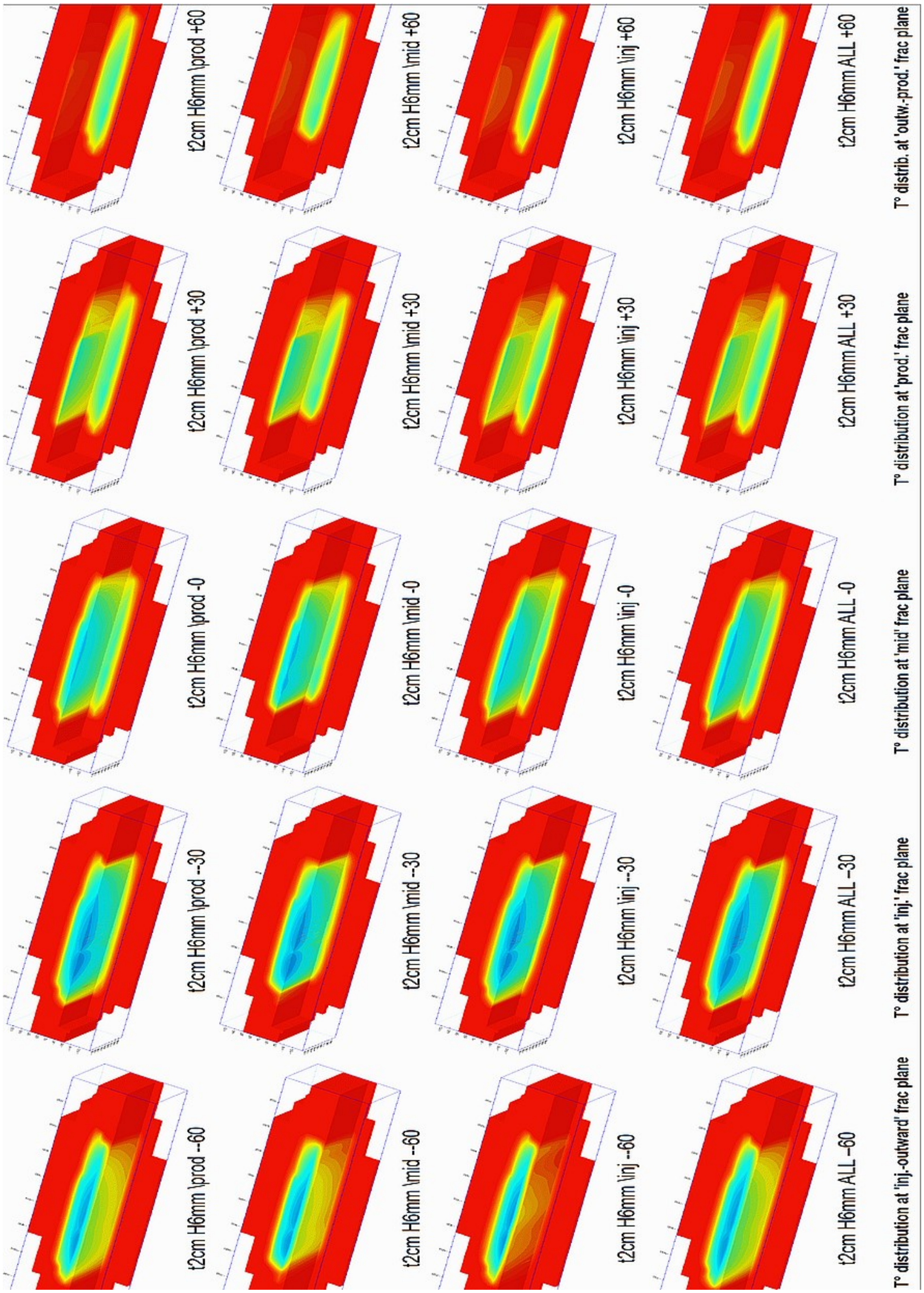

Figure 4: Heat mining effects of large-scale fractures or fault zones, obliquely 'well-aligned' to the well-doublet axis. Their overall effect on production temperature remains almost negligible, in spite of large-scale transverse 'spreading' of the cooling 'plume' along each fracture plane, and of considerable differences when one such fracture is missing. (Each row shows the temperature distribution in a fixed vertical plane, whereas each column corresponds to one missing fracture).

Owing to the petrothermal behavior thus ascertained, production temperature decline rates (fig. 2) are likely to significantly dwindle over the next decade; production temperatures would not drop below 95°C for at least 35 years under the current operation scheme. This means 'a piece of good news', along with the 'bad news' of a 'misaligned' (inter-well longitudinal) fracture being present in the reservoir.

3. RESIDENCE TIME KNOWLEDGE MINING FROM EARLY DETECTION THRESHOLDS

At the other end of the fluid residence time spectrum, one is happy to find 'large enough' natural reservoirs (not in need for stimulation or 'enhancement') but then, in turn, one has to face the challenge of "*long residence times – bad tracer tests?*" (as discussed by Behrens et al. 2021[b], Ghergut et al. 2015). As a workaround (fig. 5), relying on 'nil' signals from inter-well tracer tests at incipient stages, one can attempt to estimate lower-bounds on fluid residence times (and thus on fluid turnover volumes, a. k. a. 'reservoir sizes').

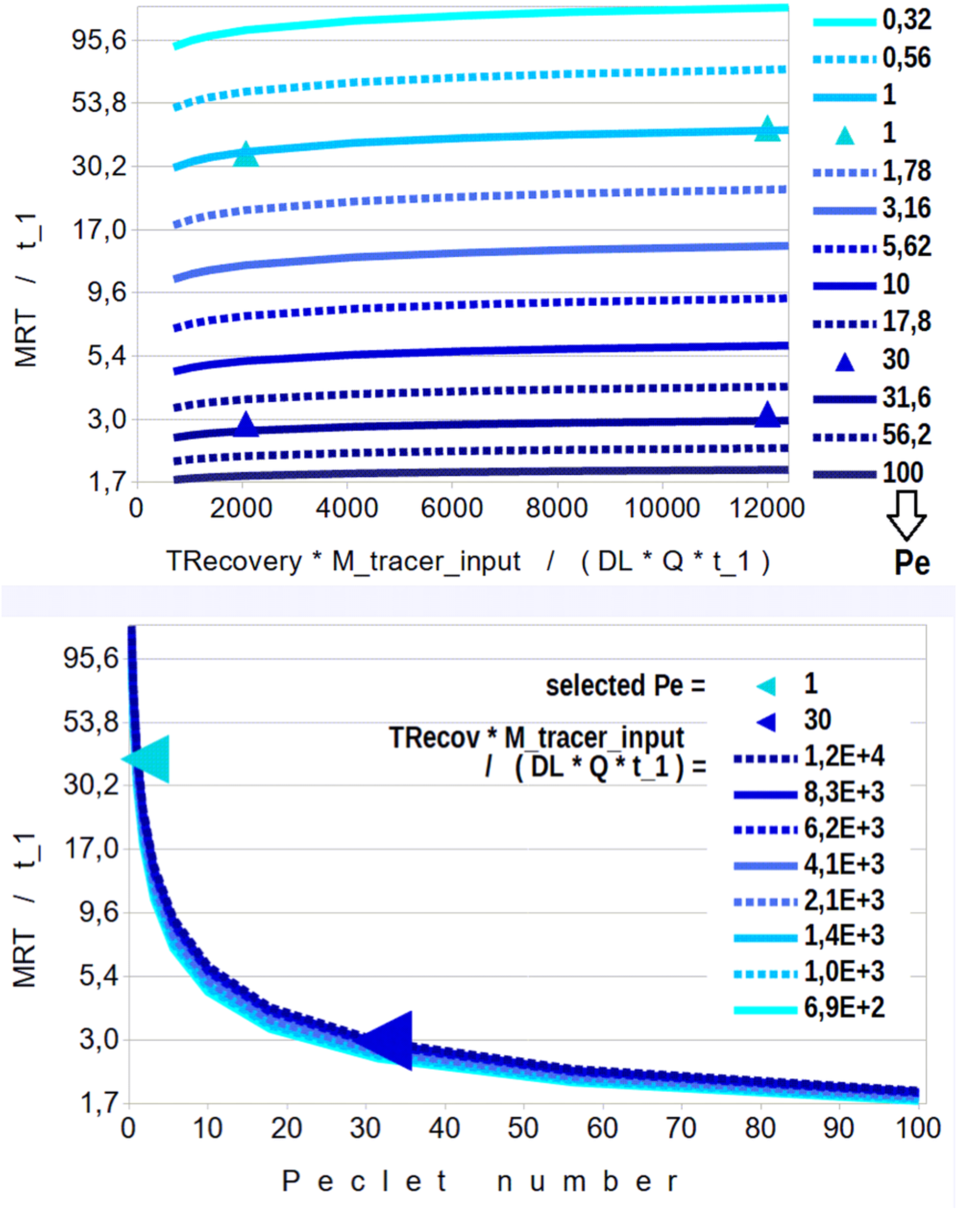

Figure 5: Monotonous correlation between the conservative tracer's so-called "first-detection time" (t_1) and the fluid's mean residence time (MRT). Upper plot: type-curve family for MRT / t_1 as a function of the assumed large-time asymptotic tracer recovery ratio (TRecov), parametrized by the Péclet number (Pe) assuming advective-dispersive transport only. Lower plot: 'quasi-universal' (approximately unique) type curve for MRT / t_1 as a function of Pe, with only slight dependency on TRecov. The scaling factor chosen for TRecov results from the ratio of two characteristic volumes ("very small" / "very large"), as explained in section 3, which accounts for abscissa (upper plot) and parameter (lower plot) values in the range of tens of thousands or higher, for most settings of practical interest (such large values are realistic).

How can one infer the fluid's (or tracer's) mean residence time (MRT) from the so-called "first-arrival time" t_1 (properly speaking, the "first-detection time"), given a specified (finite non-zero) value DL for the analytical detection limit? Inferring from t_1 to MRT is essentially model-dependent. Assuming just advective-dispersive transport for the tracer in the reservoir, fig. 5 shows type-curve families for MRT (scaled by t_1) as a function of the assumed value for the asymptotic tracer recovery ratio (TRecov). The scaling factor in the upper-plot abscissa axis, and in the lower-plot legend values, expresses the ratio between two characteristic fluid volumes of contrasting size:

► (large volume) the maximum-measurable "dilution volume" (M_tracer_input / DL)

► (small volume) the fluid turnover volume until the "first arrival" time (Q □ t_1)

which explains why the abscissa values for plotting were chosen so large (whereas TRecov can only range between 0 and 1, values between few percent and rarely more than 70% being common in real-world reservoir testing). The upper plot in fig. 5 reveals something interesting: if the ratio between the two volumes exceeds about 2 □ 10^4, the inferred MRT value becomes almost independent on the assumed value for the asymptotic recovery ratio – a very helpful finding, since the latter is highly uncertain especially at early times and may remain pretty uncertain even at late signal (tailing) times. Poor sensitivity to TRecov is also recognized from the lower plot in fig. 5, revealing the (somewhat counter-intuitive) fact that MRT / t_1 is primarily a function of the Péclet number, with only slight dependency on the assumption made for the asymptotic recovery ratio.

Furthermore, 'detection limit' DL is not a universal property of the particular tracer *species* used in the test, but depends on the detection instrument and technology 'spent' (invested) into the particular tracer *test*, as well as on reservoir fluid physico-chemistry and its pre-analytical treatment. Thus, the l.-h.s. abscissa coordinate value in the upper plot of fig. 5 can be "pushed" towards the TRecov-insensitive regime by improving the analytical detection performance, i. e., by lowering the value of DL (and of course by increasing the total tracer quantity M_tracer_input 'spent' or 'invested' into the test). These relationships are not limited to tracer transport by advective-dispersive processes, but remain valid regardless of the assumed transport model. Intuitively, this can roughly be 'explained' by treating any heterogeneous reservoir as a 'multitude' of advective transport pathways; although matrix diffusion in fractured-porous media is not reducible to a linear superposition of advective-dispersive processes, it can be approximated by such (using rather low Pe numbers, in the range of 1–2, which would actually be unacceptable for pure advection-dispersion), with acceptable errors for most settings of practical interest.

Moreover, in real-world applications, DL is not going to act like a sharply defined threshold, and the "first detection" time t_1 will not occur abruptly; the tracer signal is not "definitely undetectable" for any time t < t_1, and "suddenly becomes detectable" at t = t_1. Rather, we expect to experience a time interval (extending over days, weeks, or even months) during which the tracer signal gradually becomes detectable (with increasing clarity). This leeway in time, combined with the fact that t_1 is typically much shorter than MRT, translates into a (very) large uncertainty for MRT as a "function" of t_1. (This feels 'disppointing', but it makes sense – otherwise one would not need to continue recording a tracer signal past the t_1 "threshold", and the notion of fluid residence time *distribution* would not make sense any more.)

4. CONCLUDING REMARKS

Rendering 'hidden' fractures visible by artificial tracers parallels Shapiro's (2015) agenda of using induced (micro)seismicity to infer hydraulic properties of the subsurface (with a prominent example at the KTB site). Tracer tests are indispensable, since inferring hydraulic features from (natural and/or induced) seismicity, as well as inverting hydraulic parameters from pressure signals (McDermott et al. 2006 for the KTB site) leaves fluid transport parameters yet undetermined (cf. Ghergut et al. 2019 for further examples).

It looks somewhat spectacular to 'unveil' a markedly petrothermal behavior in a Malm aquifer province which is notoriously referred to as Germany's best hydrothermal region, by the current state of knowledge (cf. Moeck et al. 2020[a], Schumacher and Schulz 2013, Lafogler et al. 2016). Moreover, this serendipitous petrothermal reservoir development within a hydrothermal par-excellence play area appears to be the most successful (!) among all petrothermal systems whose development was attempted in Germany so far.

Along with certain non-standard observations from other sites in the Alpine foreland basin (cf. Moeck et al. 2020[b]; Stober et al. 2013; Seiler et al. 1989, 1995; Glaser 1998; Gräber 2012), especially at Geretsried within the Munich Metropolitan Region, Sankt Gallen in the Swiss Molasse Basin, and Kirchweidach in North-Eastern Bavaria, our tracer-quantified finding of a large-scale 'Malm petrothermal' system sheds a new light on carbonate-petrothermal prospects which might become worth dedicated exploration in the near future.

The late-tailing regime, accessible within affordable 'waiting time', synchronously for both tracers (in guise of endo-tracers, cf. Ghergut et al. 2019) provides the opportunity of a comparative in-situ push-pull (single-well dilution) test, to verify that rate sensitivity and flow-storage distribution shift (cf. fig. 3 of Behrens et al 2021[a]), which would be beneficial for the reservoir's thermal lifetime, is not an artifact (reflecting physico-chemical dissimilarities between the two tracer species used in the 'slow flow' and the 'rapid flow' tests), but a genuine hydrogeological feature inducing the 'dynamic response' of the Malm reservoir. Such opportunity of a 'new' tracer test without adding 'new tracer' (cf. marks in yellow on fig. 3 in section 2) is seen to occur within just few months from breakthrough peak detection (the pleasant 'flip side of the coin' to premature decline of production temperatures). Indeed a pretty rare occasion in the realm of deep-geothermal reservoirs, and of particular value for a production well, whose unnecessary 'contamination' by added tracers is to be avoided by any means.

5. ACKNOWLEDGMENTS

Fruitful cooperation with colleagues from HYDROISOTOP GmbH (Schweitenkirchen), Stadtwerke München, ERDWERK GmbH and the Technical University of Munich, as well as long-term financial support (2014 – 2021) from Germany's Federal Ministry for Economic Affairs and Energy (BMWi project "TRENDS" under grant no. / FKZ 0325515), are gratefully acknowledged.

Part of the work described in section 3 was conducted for the co-operative research project "GFK-Monitor", led by Prof. Kai Zosseder and Christine Haas at the Technical University of Munich (Hydrogeology and Geothermics Dept.) and funded by Germany's Federal Ministry for Economic Affairs and Climate Action (BMWK, under grant no. 03EE4036E).

REFERENCES

Behrens, H., Ghergut, J., Sauter, M., Wagner, B., Wiegand, B.: Premature decline of production temperature – can tracer test tell why?, Proceedings, 45th Workshop on Geothermal Reservoir Engineering, Stanford University, Stanford, CA (2020), SGP-TR-216, 195–201.

Behrens, H., Ghergut, J., Sauter, M.: First-order discontinuity in cumulative tracer recovery: need for endo-tracer push-pull, Proceedings, 46th Workshop on Geothermal Reservoir Engineering, Stanford University, Stanford, CA (2021^a), SGP-TR-218, 130–135.

Behrens, H., Ghergut, J., Sauter, M.: Non-intersected nearby faults: a blind spot for artificial tracers in inter-well tests? scoping simulations, 3, Proceedings, 46th Workshop on Geothermal Reservoir Engineering, Stanford University, Stanford, CA (2021^b), SGP-TR-218, 136–138.

Ghergut, J., Bedoya-González, D. A., Bensabat, J., McDermott, C., Wagner, B., Wiegand, B., Sauter, M.: Endo-tracer aided visibility of 'nearby' fault reactivation: scoping simulations, II, Proceedings, 44th Workshop on Geothermal Reservoir Engineering, Stanford University, Stanford, CA (2019), SGP-TR-214, 217–227.

Glaser, S.: Der Grundwasserhaushalt in verschiedenen Faziesbereichen des Malms der Südlichen und Mittleren Frankenalb, Ph. D. Thesis, published as GSF-Report 2/98, Neuherberg, Germany (1998).

Gräber, K.: Geothermieprojekt Kirchweidach – Optimierte Stimulationsmaßnahmen und Airlift-Pumpversuche, Tagungsband, Der Geothermiekongress 2012 in Karlsruhe, published by GtV-BVG (Eds.), ISBN: 978-3-932570-67-4, Berlin (2012).

Horne, R.: Reservoir engineering aspects of reinjection, Geothermics, 14 (1985), 449–457.

Lafogler, M., Wenderoth, F., Bartels, J., Somogyi, G., Hinkofer, T., Hes, K., Baumann, T.: Processes in the Vicinity of an Injection Well of a Geothermal Facility in the Malm Aquifer, Proceedings, 41st Workshop on Geothermal Reservoir Engineering, Stanford University, Stanford, CA (2016), SGP-TR-209.

Moeck, I. S., Dussel, M., Weber, J., Schintgen, T., Wolfgramm, M.: Geothermal play typing in Germany, case study Molasse Basin: a modern concept to categorise geothermal resources related to crustal permeability, Netherlands Journal of Geosciences, 98 (2020^a), doi 10.1017/njg.2019.12

Moeck, I., Straubinger, R., Thuro, K., Stockinger, G., Dussel, M.: The deep well GEN-1ST-A1 (Geretsried, Bavaria) – Unlocking a geothermal reservoir. Oil□Gas, 46/1 (2020^b), 1–3, doi 10.10225/200311

Pruess, K., and Bodvarsson, G. S.: Thermal effects of reinjection in geothermal reservoirs with major vertical fractures, Journal of Petroleum Technology, 36 (1984), 1567–1578.

Schumacher, S., and Schulz, R.: Effectiveness of acidizing geothermal wells in the South German Molasse Basin, Geothermal Energy Science, 1 (2013), 1–11.

Seiler, K.-P., Maloszewski, P., Behrens, H.: Hydrodynamic dispersion in karstified limestones and dolomites in the Upper Jurassic of the Franconian Alb, FRG, Journal of Hydrology, 108 (1989), 235–247.

Seiler, K.-P., Behrens, H., Wolf, M.: Use of artificial and environmental tracers to study storage and drainage of groundwater in the Franconian Alb, Germany, and the consequences for groundwater protection, IAEA Proceedings, Isotopes in Water Resources Management, 2 (1995), 135–146.

Shapiro, S. A.: Fluid-induced seismicity, Cambridge University Press (2015).

Stober, I., Jodocy, M., Hintersberger, B.: Gegenüberstellung von Durchlässigkeiten aus verschiedenen Verfahren im tief liegenden Oberjura des südwestdeutschen Molassebeckens, Z. Dt. Ges. Geowiss., 164 (2013), 663–679.

Ueckert, M., Wismeth, C., Baumann, T.: Crystallization of calcium carbonate in a large scale push-pull heat storage test in a jurassic carbonate aquifer, Geothermal Energy, 8 (2020), doi 10.1186/s40517-020-0160-5.